MULTIPLE SCLEROSIS JOURNAL | MSJ

Original Research Paper

Enlarged perivascular spaces are associated with brain microangiopathy and aging in multiple sclerosis

Multiple Sclerosis Journal

1–11

DOI: 10.1177/13524585241256881

Serena Borrelli*, François Guisset*, Colin Vanden Bulcke, Anna Stölting, Céline Bugli, Valentina Lolli, Renaud Du Pasquier, Vincent van Pesch, Martina Absinta, Marco Pasi* and Pietro Maggi*

Abstract

Background: Growing evidence links brain-MRI enlarged perivascular spaces (EPVS) and multiple sclerosis (MS), but their role remains unclear.

Objective: This study aimed to investigate the cross-sectional associations of EPVS with several neuroinflammatory and neurodegenerative features in a large multicentric-MS cohort.

Methods: In total, 207 patients underwent 3T axial-T2-weighted brain-MRI for EPVS assessment (EPVS dichotomized into high/low according to $\geq 2/< 2$ rating categories). MRI biomarkers included brain-predicted age and brain-predicted age difference (brain-PAD), central vein sign (CVS)-positive lesion percentage (CVS%), paramagnetic rim and cortical lesions, T2-lesion load, and brain volumetry. The variable relative importance for EPVS-category prediction was explored using a classification random forest approach.

Results: High EPVS patients were older (49 vs 44 years, $p=0.003$), had ≥ 1 vascular risk factors (VRFs; $p=0.005$), lower CVS% (67% vs 78%, $p<0.001$), reduced brain volumes (whole brain: 0.63 vs 0.73, $p=0.01$; gray matter: 0.36 vs 0.40; $p=0.002$), and older brain-predicted age (58 vs 50 years, $p<0.001$). No differences were found for neuroinflammatory markers. After adjusting for age and VFRs (multivariate analyses), the high EPVS category correlated with lower CVS% (odds ratio (OR) = 0.98, 95% confidence interval (CI) = 0.96–0.99; $p=0.02$), lower whole brain (OR = 0.01, 95% CI = 0.0003–0.5; $p=0.02$), gray matter (OR = 0.0004, 95% CI = 0.0000004–0.4; $p=0.03$) volumes, and higher brain-PAD (OR = 1.05, 95% CI = 1.01–1.09; $p=0.02$). Random forest identified brain-PAD as the most important predictor of high EPVS.

Conclusion: EPVS in MS likely reflect microangiopathic disease rather than neuroinflammation, potentially contributing to accelerated neurodegeneration.

Keywords: Enlarged perivascular spaces, multiple sclerosis, magnetic resonance imaging, brain-predicted age, cerebral small vessel disease, vascular risk factors

Date received: 1 March 2024; revised: 29 April 2024; accepted: 7 May 2024.

Correspondence to:
Pietro Maggi
Department of Neurology, Cliniques Universitaires Saint-Luc, Université catholique de Louvain, Av. Hippocrate 10, 1200 Brussels, Belgium.
pietro.maggi@uclouvain.be

Serena Borrelli
Neuroinflammation Imaging Lab (NIL), Institute of NeuroScience, Université catholique de Louvain, Brussels, Belgium/ Department of Neurology, Hôpital Erasme, Hôpital Universitaire de Bruxelles, Université Libre de Brussels, Brussels, Belgium

François Guisset
Neuroinflammation Imaging Lab (NIL), Institute of NeuroScience, Université catholique de Louvain, Brussels, Belgium

Anna Stölting
Neuroinflammation Imaging Lab (NIL), Institute of NeuroScience, Université catholique de Louvain, Brussels, Belgium

Colin Vanden Bulcke
Neuroinflammation Imaging Lab (NIL), Institute of NeuroScience, Université catholique de Louvain, Brussels, Belgium/ICTEAM Institute, Université catholique de Louvain, Louvain-la-Neuve, Belgium

Céline Bugli
Plateforme technologique de Support en Méthodologie et Calcul Statistique, Université catholique de Louvain, Brussels, Belgium

Valentina Lolli
Department of Radiology, Hôpital Erasme, Hôpital Universitaire de Bruxelles, Université Libre de Brussels, Brussels, Belgium

Renaud Du Pasquier
Neurology Service, Department of Clinical

Introduction

Perivascular spaces are small interstitial fluid-filled compartments around arterioles and venules penetrating the brain parenchyma, considered to play a critical role in the lymphatic clearance pathway and immune regulation within the central nervous system.[1] When dilated and readily visible on T2-weighted magnetic resonance imaging (MRI), these structures are referred as enlarged perivascular spaces (EPVS).[1] Although they can also be observed in healthy individuals,[2,3] EPVS are a well-recognized marker of perivascular space dysfunction, as their presence has been associated with vascular risk factors (VRFs), such as advancing age, hypertension, and other features of cerebral small vessel disease (CSVD).[4] From a physiopathological point of view, widening of the

Neurosciences, Centre Hospitalier Universitaire Vaudois, University of Lausanne, Lausanne, Switzerland

Vincent van Pesch
Department of Neurology, Cliniques Universitaires Saint-Luc, Université catholique de Louvain, Brussels, Belgium

Martina Absinta
Vita-Salute San Raffaele University, Milan, Italy/Translational Neuropathology Unit, Division of Neuroscience, IRCCS San Raffaele Scientific Institute, Milan, Italy/Department of Neurology, Johns Hopkins University School of Medicine, Baltimore, MD, USA

Marco Pasi
Stroke Unit, Department of Neurology, CIC-IT 1415, CHRU de Tours, INSERM 1253 iBrain, Tours, France

Pietro Maggi
Neuroinflammation Imaging Lab (NIL), Institute of NeuroScience, Université catholique de Louvain, Brussels, Belgium/Neurology Service, Department of Clinical Neurosciences, Centre Hospitalier Universitaire Vaudois, University of Lausanne, Lausanne, Switzerland/Department of Neurology, Cliniques Universitaires Saint-Luc, Université catholique de Louvain, Brussels, Belgium

*Serena Borrelli, François Guisset, Marco Pasi and Pietro Maggi contributed equally to this article.

brain perivascular spaces in CSVD is likely to result from fluid drainage obstruction and liquid stagnation secondary to hypoxia, inflammation, vascular remodeling, and endothelial dysfunction.[5] However, the exact sequence of event leading to MRI visible EPVS in CSVD and other brain disorders is yet to be determined.

Accumulating evidence suggests a higher EPVS burden in multiple sclerosis (MS), but their exact clinical and pathophysiological significance remains controversial.[6] While previous studies have inconsistently[6] associated EPVS with active MS neuroinflammation[7,8] and brain volume loss,[9] recent findings suggest a potential link between EPVS and vascular comorbidities. In fact, we have recently described that in MS patients with vascular comorbidities, an increased count of EPVS in the centrum semiovale (CSO) is associated with a lower percentage of MS-specific perivenular lesions.[10] Furthermore, a post-mortem MRI-pathology correlation study observed that EPVS did not colocalize at the anatomical level with common MS pathological features, such as perivenular demyelination and immune cell infiltration, but rather with small arterial blood vessels.[11]

By addressing these research gaps, we aimed to better characterize EPVS as a clinically relevant imaging biomarker in MS, by investigating its cross-sectional association with several clinical and MRI features of neuroinflammation and neurodegeneration in a large multicentric cohort of patients with MS.

Methods

Study population

Patients with a diagnosis of clinically isolated syndrome (CIS), relapsing–remitting (RRMS), secondary progressive (SPMS), or primary progressive (PPMS) MS, according to the 2017 McDonald criteria[12] were enrolled between October 2016 and March 2023 from three academic research hospitals: Erasme University Hospital (Brussels, Belgium), Saint-Luc University Hospital (Brussels, Belgium), and Lausanne University Hospital (Lausanne, Switzerland). Study approval was given from an ethical standard committee on human experimentation in each hospital, and written informed consent was obtained from all subjects.

The inclusion criteria were the following: (1) age $\geq$ 18 years, availability of 3-Tesla (3T) (2) T2-weighted turbo spin echo (TSE), for the EPVS assessment, and (3) three-dimensional (3D) segmented T2*-weighted echo-planar imaging (EPI), for central vein sign (CVS) assessment. Exclusion criteria included suboptimal MRI image quality due to motion artifact.

MRI acquisition protocol

MRI studies were performed on four 3T MRI scanners: Philips Ingenia scanners (Philips Medical Systems, The Netherlands—Erasme University Hospital), Siemens Skyra or Prisma scanners (Siemens AG, Germany—Lausanne University Hospital), and General Electric Signa Premier (GE Healthcare, Waukesha, Wisconsin, USA—Saint-Luc University Hospital). However, 3T MRI protocol included a T2-weighted TSE for the EPVS assessment and a submillimeter isotropic 3D-segmented T2*-weighted EPI sequence[13–15] for the detection of both CVS and paramagnetic rim lesions (PRL). Cortical lesion (CL) assessment was performed on 3D double inversion recovery (DIR)[16] or 3D-synthetic DIR (generated from T1/T2 images)[17] and 3D T1-weighted magnetization-prepared rapid gradient echo images (MPRAGE).[16,18] Additional MRI methods are detailed in the Supplementary Methods and Supplementary Table 1.

Image processing and biomarker assessment

Given that raters were partially involved in the recruitment of cases, all images were de-identified before analysis.

EPVS were assessed according to previously published guidelines.[19] We used a validated four-point visual rating scale (0 = no EPVS, 1 = < 10 EPVS, 2 = 11–20 EPVS, 3 = 21–40 EPVS, and 4 = > 40 EPVS) to score EPVS on the axial T2-TSE images at the level of the centrum semiovale (CSO-EPVS) and the basal ganglia (BG-EPVS). T2-FLAIR images were used to differentiate EPVS from hyperintense lesions or lacunes.[20] Depending on the distribution in our cohort and a previously published threshold,[3,21] we further dichotomized EPVS scores as "high" and "low" based on a $\geq$ 2 EPVS score threshold which allowed a balanced group sizes.

Brain-predicted ages were calculated using BrainageR software v2.1 (https://github.com/jamescole/brainageR) as previously described.[22,23] This software takes as input raw, unprocessed MPRAGE images, and then performs image normalization and segmentation via SPM12 (https://www.fil.ion.ucl.ac.uk/spm/software/spm12/) to generate volumes for gray

matter, white matter, and cerebrospinal fluid. The vectorized images are then applied to a Gaussian Process Regression model to predict brain age. Based on the brain-predicted age, the brain-predicted age difference (brain-PAD) was finally calculated by subtracting the chronological age from the brain-predicted age of each subject. A positive brain-PAD indicates « accelerated » brain aging compared to the chronological age, whereas a negative value suggests a « delayed » brain aging.

For the CVS analysis, the percentage of perivenular lesions across all eligible brain lesions[24] was determined in each participant, hereafter termed "proportion of CVS-positive lesions." In this specific study, the proportion of CVS-positive lesions was considered as surrogate biomarker of microischemic lesion burden since a higher proportion of CVS-negative microangiopathic MRI lesions corresponds to a lower proportion of CVS-positive demyelinating lesions.[10] For PRL analysis, both the total PRL number and the PRL 0–4 versus >4 categories were established in each subject. The categories were based on a previously proposed clinically meaningful threshold of four PRL per patient,[25] and on the distribution of our cohort data. For CL analysis, the total CL number was used. The CVS, and PRL and CL assessments were performed following previously published guidelines and methods; see Supplementary Methods for details.[16,24,26,27]

Brain volumes normalized to intracranial volume and total white matter T2-hyperintense lesion volume (hereafter, "T2 lesion load") were also computed; see the Supplementary Methods for details.

In each individual, EPVS, CVS, PRL, and CL analysis were independently assessed by two trained investigators (F.G. and M.P. for EPVS assessment, S.B. and F.G. for CVS assessment, P.M. and M.A. for PRL assessment, A.S. and S.B. for CL assessment), each unaware of the other's analysis. In case of discrepancies, the scans were jointly reviewed by the two investigators to reach a consensus.

Clinical assessment

Demographic and clinical data were recorded for each patient. The MS disability (Expanded Disability Status Scale (EDSS)) and severity (Multiple Sclerosis Severity Scale (MSSS)) scales were obtained from experienced MS clinicians at the time of the research MRI scan. The presence/absence of the following VRFs for CSVD was recorded for each patient:[28–30] (1) arterial hypertension (AHT), that is, established diagnosis and treatment with at least one antihypertensive drug; (2) Type 1 or Type 2 diabetes (diabetes), that is established diagnosis and treatment with at least one antidiabetic drug; (3) smoking, current or former; (4) obesity (BMI $\geqslant 30\,kg/m^2$); and (5) hypercholesterolemia, that is, established diagnosis and treatment with at least one hypolipemic drug. A cumulative VRFs score was then calculated.

Statistical analysis

Demographic, clinical, and MRI comparisons were assessed with independent sample Student's *t*, Mann–Whitney U test, chi-square or Fisher's exact tests, when appropriate. The Benjamini–Hochberg procedure was applied to control the false discovery rate (FDR) across all tested hypotheses when correcting for multiple comparisons.

The interrater reliability for EPVS, CVS, PRL, and CL assessment was explored on a per-patient level using the one-way random model intraclass correlation coefficient (ICC).[31]

The association between the EPVS categories (dependent variable) and all significant clinical and MRI variables from univariate tests (independent variables) were further explored using logistic binomial regression models. To compare model fit, a likelihood ratio test was conducted to evaluate whether the addition of predictors significantly improved the model.

To exclude any possible influence of the different 3T scanners on the results, we repeated all analyses adding "MRI center" as covariate.

The relative importance of all significant clinical and MRI variables from univariate tests was finally explored fitting a random forest model to predict EPVS categories. The random forest model was implemented using the randomForest R package with 500 trees, and the dataset was randomly split into training (70%) and testing (30%) sets for model training and evaluation, respectively. Model performance was measured by the area under the receiver operating characteristic curve (AUC) and mean decrease Gini (MDG) importance measure.

Statistical analyses were performed with IBM SPSS Statistics (version 29.0.1.0) and RStudio (version 2023.06.1 + 524). Statistical significance was considered when p-value was less than 0.05.

Table 1. EPVS rating score at the level of the centrum semiovale (CSO-EPVS) and the basal ganglia (BG-EPVS).

	Grade 0	Grade 1	Grade 2	Grade 3	Grade 4
CSO-EPVS, *n* (%)	–	128 (61.8)	61 (29.5)	15 (7.2)	3 (1.4)
BG-EPVS, *n* (%)	–	194 (93.7)	11 (5.3)	2 (1.0)	–

Results

Demographic and clinical data

In total, 207 patients (63% female) with MS were included in this analysis (6% CIS, 55% RRMS, 26% SPMS, and 13% PPMS).

The ICC interrater agreement for EPVS, CVS, PRL, and CL assessment was 0.877 ($p < 0.001$), 0.995 ($p < 0.001$), 0.998 ($p < 0.001$), and 0.986 ($p < 0.001$), respectively.

EPVS rating scores at the level of CSO and BG are described in Table 1. No EPVS rating score of 0 was observed. A high CSO-EPVS score was found in 38.2% (low CSO-EPVS score in 61.8%). Since a high BG-EPVS score was found only in 6.3% (low BG-EPVS score in 93.7%), further analyses focused on CSO-EPVS only. Clinical and MRI features of patients with high and low EPVS scores are reported in Tables 2 and 3, respectively.

When we tested the influence of the different 3T scanners on EPVS score detection rate, after correcting by age and sex, we did not find an association between a high CSO-EPVS score and "MRI center" (Supplementary Table 2).

EPVS is associated with microischemic lesion burden

When cases with high CSO-EPVS score were compared to those with low CSO-EPVS score, the median proportion of CVS-positive lesions was lower in the first group (67% vs 78%, $p < 0.001$; Table 3 and Figure 1). This was confirmed by the regression model where, after adjusting for age, a high CSO-EPVS score was associated with a lower proportion of CVS-positive lesions (odds ratio (OR) 0.98, 95% confidence interval (CI) 0.96–0.99; $p = 0.024$). The addition of AHT and hypercholesterolemia as additional predictors did not significantly improve the model (deviance difference = 3.93, $df = 2$, $p = 0.14$). Also, after adding "MRI center" as covariate, a high CSO-EPVS score was still associated with a lower proportion of CVS-positive lesions (Supplementary Table 3).

EPVS is not associated with MS inflammatory activity nor clinical disability and severity

No differences were found in cases with high CSO-EPVS compared to those with low CSO-EPVS score for all the demyelinating inflammatory biomarkers studied (presence of $\geqslant 1$ MS relapse in the previous year, $p = 0.40$; presence of MRI gadolinium-enhancing lesions, $p = 0.58$; number of PRL, $p = 0.81$; presence of > 4 PRL, $p = 0.72$; number of CL, $p = 0.61$; presence of CSF-restricted oligoclonal bands at diagnosis, $p = 0.58$). Similarly, clinical disability (EDSS; $p = 0.77$) and severity (MSSS; $p = 0.56$) scores did not differ between MS cases with a high CSO-EPVS versus those with a low CSO-EPVS score (Tables 2 and 3).

EPVS is associated with brain volumes and brainage

Lower median normalized whole brain (0.633 vs 0.729; $p = 0.011$) and gray matter (0.355 vs 0.400; $p = 0.002$) volumes were found in cases with high CSO-EPVS compared to those with low CSO-EPVS scores (Table 3). After controlling for age, AHT, and hypercholesterolemia, patients with a high CSO-EPVS score had a reduced whole brain (OR 0.01, 95% CI: 0.0003–0.5; $p = 0.02$) and gray matter (OR 0.0004, 95% CI: 0.0000004–0.4; $p = 0.03$) volume compared to patients with a low CSO-EPVS score.

An older brain-predicted age was found in cases with a high CSO-EPVS compared to those with a low CSO-EPVS score (58 vs 50 years; $p < 0.001$; Table 3 and Figure 2). To assess whether brain-predicted age contained information beyond chronological age, the brain-PAD was assessed in each patient. After controlling for age, AHT, and hypercholesterolemia, the multivariate regression model revealed a significant association between a positive brain-PAD and high CSO-EPVS score (OR 1.05, 95% CI 1.01–1.09; $p = 0.021$). After adding "MRI center" as covariate, a high CSO-EPVS score was still associated with higher positive brain-PAD (Supplementary Table 4).

Random forest for EPVS prediction

When all significant clinical and MRI variables associated to CSO-EPVS scores (Tables 2 and 3) were

Table 2. Clinical data in patients with high and low CSO-EPVS score.

Characteristic	CSO-EPVS			
	High ($n=79$)	Low ($n=128$)	p	Adjusted p (FDR)
Women, n (%)	50 (63.3)	79 (62.2)	χ^2 n.s.	n.s.
Age, years, mean (range)	49 (20–75)	44 (22–73)	Student's t, $p=$**0.003**	$p=$**0.02**
Disease phenotype, n (%)				
- CIS	3 (3.8)	9 (7.0)	Fisher n.s.	n.s.
- RRMS	46 (58.2)	68 (53.1)	χ^2 n.s.	n.s.
- SPMS	20 (25.3)	33 (25.8)	χ^2 n.s.	n.s.
- PPMS	10 (12.7)	18 (14.1)	χ^2 n.s.	n.s.
EDSS, median (range)	2.5 (0–7.0)	2.5 (0–7.5)	Mann–Whitney n.s.	n.s.
MSSS, median (range)	4.27 (0.13–9.08)	4.35 (0.05–9.84)	Mann–Whitney n.s.	n.s.
$\geqslant 1$ relapse in the previous year, n (%)	8 (26.7)	25 (35.2)	χ^2 n.s.	n.s.
Disease duration, years, median (range)	8.8 (0–41.9)	6.3 (0–39.9)	Mann–Whitney, $p=$**0.025**	n.s.
OCBs presence at diagnosis ($n=164$), n (%)	55 (87.3)	85 (84.2)	χ^2 n.s.	n.s.
AHT, n (%)	17 (21.8)	11 (8.9)	χ^2 $p=$**0.01**	$p=$**0.048**
Diabetes, n (%)	5 (6.4)	5 (4.1)	χ^2 n.s.	n.s.
BMI $\geqslant 30\,kg/m^2$, n (%)	11 (16.7)	9 (9.5)	χ^2 n.s.	n.s.
Smoking, n (%)	24 (45.3)	28 (39.4)	χ^2 n.s.	n.s.
Hypercholesterolemia, n (%)	20 (26.3)	16 (13.2)	χ^2 $p=$**0.021**	n.s.
Cumulative no. of VRFs, median (range)	1 (0–5)	0 (0–4)	Mann–Whitney $p=$**0.005**	$p=$**0.03**

AHT: arterial hypertension; BMI: body mass index; CIS: clinically isolated syndrome; EDSS: expanded disability status scale; EPVS: enlarged perivascular spaces; FDR: False Discovery Rate; MSSS: multiple sclerosis severity score; OCBs: CSF-restricted oligoclonal bands; PPMS: primary progressive multiple sclerosis; RRMS: relapsing–remitting multiple sclerosis; SPMS: secondary progressive multiple sclerosis; VRFs: vascular risk factors.
Significant p values ($p<0.05$) are highlighted in bold.

combined in a random forest model, the variable importance analysis revealed that the most important predictors for high EPVS score were brain-PAD, followed by normalized whole brain volume, age, percentage of CVS-positive lesions, and normalized gray matter volume, while the cumulative number of VRFs, hypercholesterolemia, and AHT showed the least importance (Table 4).

Discussion

In this cross-sectional multicenter academic study, we explored the role of EPVS as a clinically relevant imaging biomarker in MS, by investigating their relationship with several clinical and MRI markers of neuroinflammation and neurodegeneration. We found that EPVS in MS were more frequently observed in the CSO and were associated with brain microangiopathy more than brain inflammation since a lower proportion of CVS-positive lesions was found in patients with higher EPVS rating score and no associations were found with any of the clinical and MRI inflammatory demyelinating features explored. Moreover, a higher EPVS burden correlated with lower whole brain and gray matter volumes—and with an older brain-predicted age—suggesting a potential role of EPVS as a surrogate marker of neurodegeneration in MS.

Accumulating evidence has shown a high EPVS burden in patients with MS,[6] but the exact clinical and pathophysiological significance of this MRI biomarker in the disease remains a matter of debate. Given the role of perivascular spaces in leukocyte trafficking and modulation of immune responses,[32,33] it has been suggested that EPVS in MS may reflect perivascular inflammation during the formation of demyelinating lesions.[8,34] However, in agreement with recent evidences from the literature,[6,11] our multicenter study did not show any difference in terms of acute (i.e. contrast-enhancing and T2 lesion load) and

Table 3. MRI data in patients with high and low CSO-EPVS score.

Characteristic	CSO-EPVS			
	High ($n=79$)	Low ($n=128$)	p	Adjusted p (FDR)
% CVS-positive lesions, median (range)	67 (23–100)	78 (0–100)	Mann–Whitney, $p<$ **0.001**	$p=$ **0.01**
Number of PRL, median (range)	1 (0–31)	1 (0–82)	Mann–Whitney n.s.	n.s.
Cases with >4 PRLs, n (%)	12 (15.4)	22 (17.3)	χ^2 n.s.	n.s.
Number of CL, median (range)	3 (0–101)	4 (0–92)	Mann–Whitney n.s.	n.s.
T2 lesion load, cm^3, median (range)	6.64 (0.13–60.5)	5.12 (0.00001–40.2)	Mann–Whitney n.s.	n.s.
Presence of Gd-enhancing lesions, n (%)	14 (17.7)	19 (14.8)	χ^2 n.s.	n.s.
Normalized whole brain volume, median (range)	0.633 (0.423–0.781)	0.729 (0.484–0.833)	Mann–Whitney $p=$ **0.011**	$p=$ **0.048**
Normalized gray matter volume, median (range)	0.356 (0.240–0.437)	0.400 (0.272–0.474)	Mann–Whitney $p=$ **0.002**	$p=$ **0.02**
Normalized thalamic volume, median (range)	0.008 (0.005–0.011)	0.008 (0.005–0.011)	Student's t n.s.	n.s.
Brain-predicted age, years, mean (range)	58 (28–84)	50 (27–79)	Student's t, $p<$ **0.001**	$p=$ **0.01**

CL: cortical lesion; CVS: central vein sign; EPVS: enlarged perivascular spaces; FDR: False Discovery Rate; Gd: gadolinium; PRLs: paramagnetic rim lesions.
Significant p values ($p<0.05$) are highlighted in bold.

more chronic/smoldering (i.e. PRL and CL counts) inflammatory activity in patients with MS and high compared to low EPVS scores.

In agreement with these findings, and confirming our previous results in a smaller MS cohort,[10] here we show that higher EPVS scores are associated with a significant decrease in the percentage of MS-specific perivenular lesions. We also found a significant correlation of the patient's cumulative number of VRFs with the EPVS burden. More specifically, older age, hypertension, and hypercholesterolemia were all associated with higher EPVS scores, all of which are well-defined risk factors for CSVD.[35] Vascular comorbidities are prevalent in MS and are associated with higher MRI microangiopathic brain lesion load.[36,37] The pathophysiology underlying brain white matter lesion formation in CSVD is believed to reflect several mechanisms, including brain hypoperfusion, reduced vascular reactivity, and tissue hypoxia, mostly occurring at the arteriolar side of the microcirculation.[37–39] Conversely, most focal inflammatory demyelinating lesions in MS develop around small parenchymal veins.[40] Our results showing that the percentage of CVS-positive lesions in MS decreases in the presence of higher EPVS burden are in line with previous studies[10,41,42] and point toward an EPVS role in microangiopathic more than demyelinating inflammatory processes in MS. As suggested by a recent post-mortem MRI-pathology study,[11] EPVS in MS are a marker for arterial disease rather than inflammatory perivenular demyelination since they colocalize with histopathological signs of arteriolar damage.[11] Even though age and other VRFs are classically associated to CSVD,[35] and the percentage of CVS-negative microangiopathic lesions increases with age,[43] our analyses clearly showed that the association between EPVS and microangiopathic CVS-negative lesions burden in MS is independent from age and other VRFs.

In agreement with previous evidence,[9,44] we found that EPVS in MS are more frequently found at the level of the CSO, while in CSVD non-MS patients, EPVS are generally most prominent in the BG.[45] Altogether, these results suggest that the physiopathology of microangiopathy in MS may be different

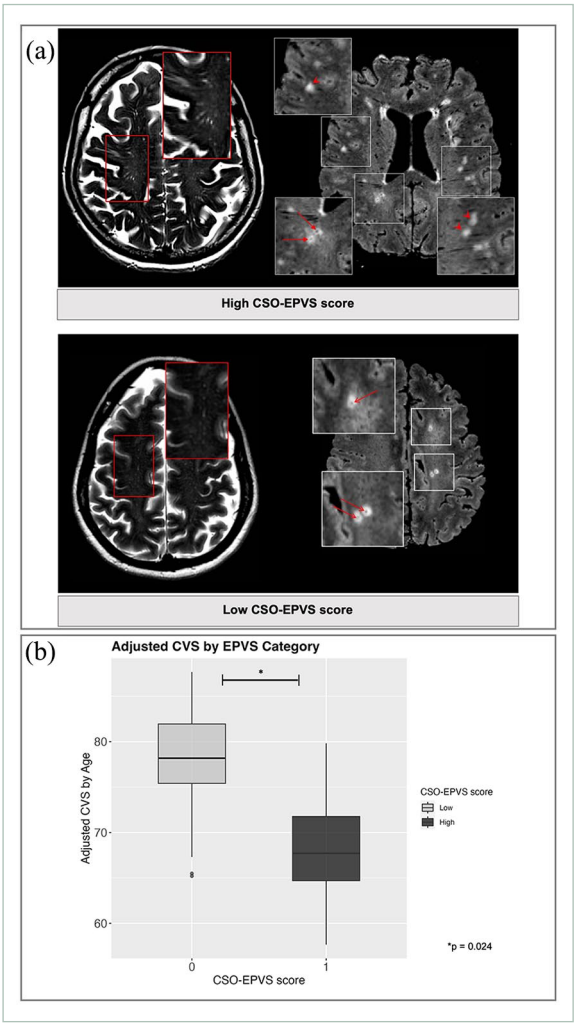

Figure 1. Percentage (%) of CVS-positive lesions in patients with MS and a high versus low CSO-EPVS rating score. (a) Upper panel: 66-year-old SPMS patient with AHT, showing prominent enlarged perivascular spaces (red magnified box) on T2-weighted images (CSO-EPVS rating score = 3), and typical MS perivenular (arrows) but also non-perivenular (arrowheads) lesions on FLAIR* images (% of CVS-positive lesions = 66%). Lower panel: 50-year-old RRMS patient without any VRFs for CSVD showing only few enlarged perivascular spaces on T2-weighted images (CSO-EPVS rating score = 1) and a high percentage of MS typical perivenular lesions (arrows) on FLAIR* images (% of CVS-positive lesions = 100%). (b) Lower % of CVS-positive lesions (adjusted by age) in cases with a high CSO-EPVS compared to those with a low CSO-EPVS score.

from the one of classical CSVD,[46] and that the chronic MS inflammatory milieu could facilitate the arteriolar damage through oxidative stress and pro-atherogenic Th1 immune response.[46,47] Future studies focusing on glymphatic system[48] might help to better understand the perivascular dysfunction in MS.

Previous studies have shown that in MS, the presence of VRFs is associated with accelerated brain volume loss and steeper cognitive decline.[36,49] In this context, brain-predicted age calculation by machine learning analysis has been extensively investigated in recent years as a marker of accelerated brain aging.[50] In MS, an increase in brain-predicted age is related to higher disability[51] and cognitive decline[52] and may also be predictive of future disability progression.[51,53] Here, we show a positive association between EPVS burden and accelerated brain aging (expressed by higher positive brain-PAD), independently from age and other VRFs. Moreover, and in agreement with one previous ultra-high field MRI study,[9] we report a significant decrease in the whole brain and gray matter volumes in MS patients with a high EPVS score. Altogether, our findings suggest that brain microangiopathy plays a significant role in MS-related neurodegeneration. Even though we can hypothesize that EPVS in MS could also be secondary to focal ex vacuo atrophy and demyelination of adjacent brain tissue,[45,54] higher EPVS burden has been inconsistently[6] associated with lower brain volume measures,[9] and a recent meta-analysis[55] did not identify a significant (negative) correlation between EPVS and brain volume. Phenomena beyond mere tissue loss, such as microangiopathy and other vascular-related factors, may contribute to the observed association between EPVS and accelerated brain aging in our cohort, highlighting the complex interplay between vascular pathology and neurodegeneration in MS.

This study has some limitations. First, EPVS were visually assessed and ordinally scored on 2D slices, which could have led to an underestimation of EPVS score compared to the quantification on 3D approach. Interrater reliability was reasonable (ICC of 0.88), but future studies should ideally use 3D acquisitions for taking advantage of recently developed algorithms[56,57] for automated quantification of EPVS exact number and volume. Second, the availability of cognitive scales would have allowed a more accurate evaluation of EPVS clinical impact. Third, given the cross-sectional design of the study, we did not dispose of longitudinal data necessary to provide information on the relevance of EPVS for predicting future MS physical or cognitive disease progression. In addition, our study adopted an exploratory approach rather than a confirmatory one, as we did not predefine the associations under investigation. Moreover, we missed an age-matched control group that would have strengthened our findings. Finally, when comparing our findings with the ones of Wuerfel et al.,[8] one should consider that this study included a large number of well-treated patients with an overall stable disease course.

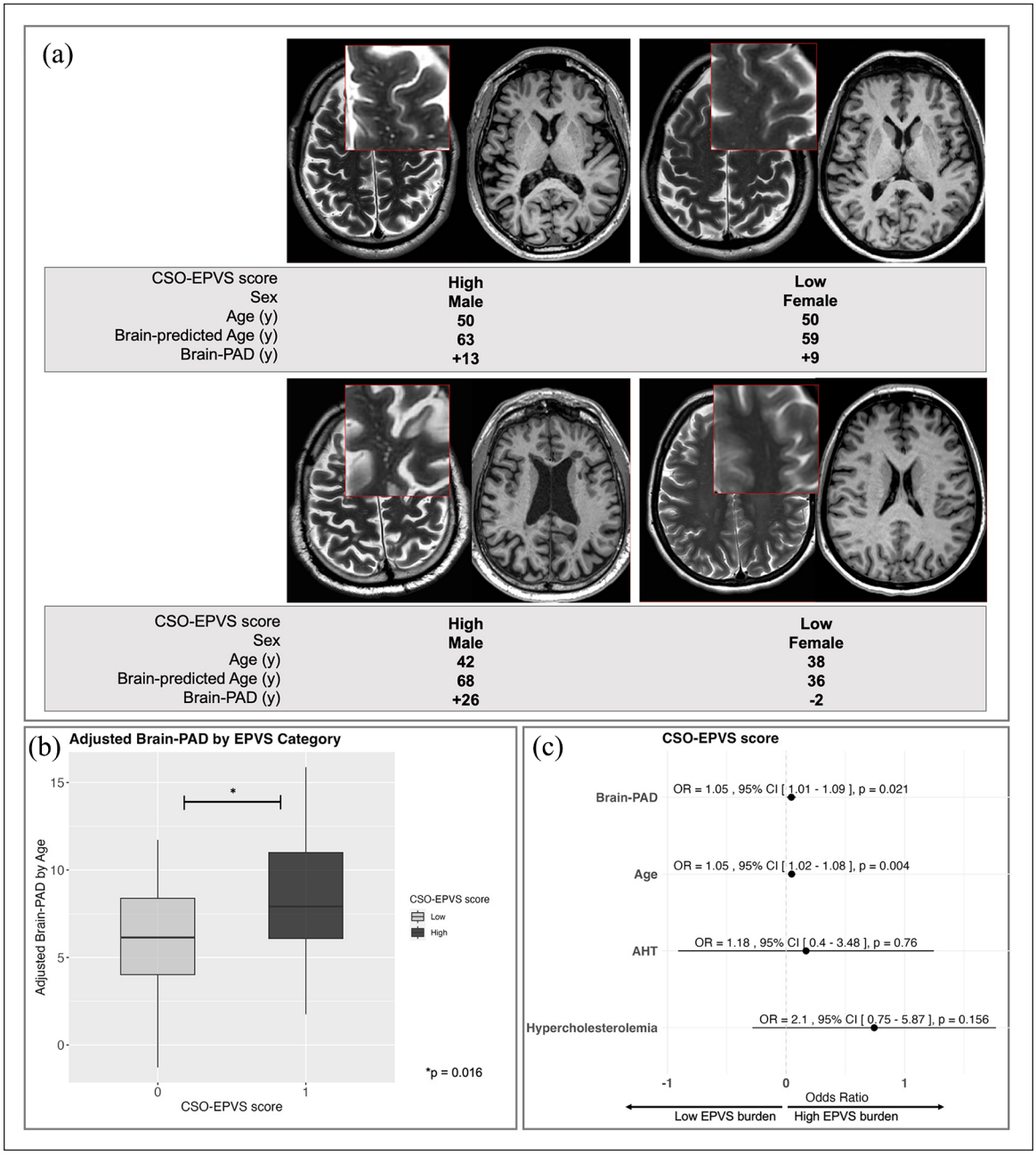

Figure 2. Brain-PAD of patients with MS and a high versus low CSO-EPVS rating score. (a) Examples of how brain structures relates to CSO-EPVS rating score and brain-PAD, with axial slices of T2-weighted images and 3D T1-weighted MPRAGE. (b) Higher positive brain-PAD (adjusted by age) in cases with a high CSO-EPVS compared to those with a low CSO-EPVS score. (c) Significant association between a positive brain-PAD and high CSO-EPVS score, after controlling for age, AHT, and hypercholesterolemia.

In conclusion, EPVS are frequent in MS and are associated with lower proportion of perivenular MS-specific lesions, with accelerated brain atrophy and brain aging. Our findings indicate that EPVS in MS can serve as surrogate biomarker of coexisting microangiopathic disease and are likely to contribute to neurodegeneration in patients with MS. Future longitudinal studies should concentrate on exploring the potential prognostic value of EPVS in MS and whether pharmacological interventions may reduce MS microangiopathic burden with an impact on clinical and MRI measures of neurodegeneration.

Table 4. Random forest informative predictors of high CSO-EPVS score.

Outcome	Predictor	Importance (MDG)	AUC (95% CI)
High CSO-EPVS score	Brain-PAD	4.33	0.81 (0.74–0.88)
	Normalized whole brain volume	3.74	
	Age	3.57	
	Normalized gray matter volume	3.45	
	% CVS-positive lesions	3.34	
	Cumulative number of VRFs	1.05	
	Hypercholesterolemia	0.24	
	AHT	0.17	

AUC: area under the receiver operating characteristic curve; Brain-PAD: brain-predicted age difference; CI: confidence interval; CVS: central vein sign; MDG: mean decrease Gini; VRFs: vascular risk factors.

Acknowledgements

The authors thank the study participants; Thierry Duprez, Sébastien de Laever (Cliniques universitaires Saint-Luc), Laurence Dricot (Université catholique de Louvain), and Julie Poujol (GE Healthcare) for assistance with 3T MRI scan acquisition and analysis.

Data Availability Statement

The data that support the findings of this study are controlled by the respective centers and are not publicly available. Written requests for access to the derived data will be considered by the corresponding author. Anonymized data will be shared by reasonable request from the principal investigator.

Declaration of Conflicting Interests

The author(s) declared the following potential conflicts of interest with respect to the research, authorship, and/or publication of this article: S.B. received speaker/consulting honoraria from Sanofi, Roche, Janssen, Merck, and Novartis, and research grants from Roche, Sanofi, and Brugmann Foundation not related to this work. F.G., C.V.B., A.S., C.B., R.D.P., V.L., and M.P. report no disclosures relevant to the manuscript. V.V.P. received consulting honoraria from Biogen, Merck, Sanofi, Bristol Myers Squibb (BMS), Novartis, Janssen, Almirall, Roche, and Alexion. M.A. received consulting honoraria from Sanofi, GSK, Biogen, Immunic Therapeutics, and Abata Therapeutics. P.M. received consulting honoraria from Sanofi, Biogen, and Merck.

Funding

The author(s) disclosed receipt of the following financial support for the research, authorship, and/or publication of this article: S.B. is supported by the Funds Claire Fauconnier, Ginette Kryksztein & José and Marie Philippart-Hoffelt, managed by the King Baudouin Foundation. C.V.B. and A.S. have the financial support of the Fédération Wallonie Bruxelles—Fonds Spéciaux de Recherche (F.S.R.). M.A. received research support from the Conrad N. Hilton Foundation (17313), the Cariplo Foundation (2019-1677), the Roche Foundation, the FRRB Early Career Award (1750327), the National MS Society (NMSS-RFA 2203-39325), and the International Progressive MS Alliance (PA-2107-38081). P.M. research activity is supported by the Fondation Charcot Stichting Research Fund 2023, the Fund for Scientific Research (F.R.S, FNRS; grant no. 40008331), Cliniques universitaires Saint-Luc "Fonds de Recherche Clinique," and Biogen.

ORCID iDs

Serena Borrelli https://orcid.org/0000-0002-3186-1562

François Guisset https://orcid.org/0000-0001-5035-0840

Pietro Maggi https://orcid.org/0000-0003-1697-5585

Supplemental Material

Supplemental material for this article is available online.

References

1. Ineichen BV, Okar SV, Proulx ST, et al. Perivascular spaces and their role in neuroinflammation. *Neuron* 2022; 110(21): 3566–3581.

2. Adams HH, Hilal S, Schwingenschuh P, et al. A priori collaboration in population imaging: The Uniform Neuro-Imaging of Virchow-Robin Spaces Enlargement consortium. *Alzheimers Dement (Amst)* 2015; 1(4): 513–520.
3. Doubal FN, MacLullich AM, Ferguson KJ, et al. Enlarged perivascular spaces on MRI are a feature of cerebral small vessel disease. *Stroke* 2010; 41(3): 450–454.
4. Wardlaw JM, Benveniste H, Nedergaard M, et al. Perivascular spaces in the brain: Anatomy, physiology and pathology. *Nat Rev Neurol* 2020; 16(3): 137–153.
5. Brown R, Benveniste H, Black SE, et al. Understanding the role of the perivascular space in cerebral small vessel disease. *Cardiovasc Res* 2018; 114(11): 1462–1473.
6. Granberg T, Moridi T, Brand JS, et al. Enlarged perivascular spaces in multiple sclerosis on magnetic resonance imaging: A systematic review and meta-analysis. *J Neurol* 2020; 267(11): 3199–3212.
7. Ge Y, Law M, Herbert J, et al. Prominent perivenular spaces in multiple sclerosis as a sign of perivascular inflammation in primary demyelination. *AJNR Am J Neuroradiol* 2005; 26(9): 2316–2319.
8. Wuerfel J, Haertle M, Waiczies H, et al. Perivascular spaces—MRI marker of inflammatory activity in the brain. *Brain* 2008; 131(Pt9): 2332–2340.
9. Kilsdonk ID, Steenwijk MD, Pouwels PJ, et al. Perivascular spaces in MS patients at 7 Tesla MRI: A marker of neurodegeneration. *Mult Scler* 2015; 21(2): 155–162.
10. Guisset F, Lolli V, Bugli C, et al. The central vein sign in multiple sclerosis patients with vascular comorbidities. *Mult Scler* 2021; 27(7): 1057–1065.
11. Ineichen BV, Cananau C, Plattén M, et al. Dilated Virchow-Robin spaces are a marker for arterial disease in multiple sclerosis. *eBioMedicine* 2023; 92: 104631.
12. Thompson AJ, Banwell BL, Barkhof F, et al. Diagnosis of multiple sclerosis: 2017 revisions of the McDonald criteria. *Lancet Neurol* 2018; 17(2): 162–173.
13. Sati P, George IC, Shea CD, et al. FLAIR*: A combined MR contrast technique for visualizing white matter lesions and parenchymal veins. *Radiology* 2012; 265(3): 926–932.
14. Sati P, Thomasson DM, Li N, et al. Rapid, high-resolution, whole-brain, susceptibility-based MRI of multiple sclerosis. *Mult Scler* 2014; 20(11): 1464–1470.
15. Absinta M, Sati P, Fechner A, et al. Identification of chronic active multiple sclerosis lesions on 3T MRI. *AJNR Am J Neuroradiol* 2018; 39(7): 1233–1238.
16. Filippi M, Preziosa P, Banwell BL, et al. Assessment of lesions on magnetic resonance imaging in multiple sclerosis: Practical guidelines. *Brain* 2019; 142(7): 1858–1875.
17. Manning AR, Beck ES, Schindler MK, et al. T 1 /T 2 ratio from 3T MRI improves multiple sclerosis cortical lesion contrast. *J Neuroimaging* 2023; 33(3): 434–445.
18. Kober T, Granziera C, Ribes D, et al. MP2RAGE multiple sclerosis magnetic resonance imaging at 3 T. *Invest Radiol* 2012; 47(6): 346–352.
19. Potter G, Morris Z and Wardlaw J. *"Enlarged perivascular spaces (EPVS): A visual rating scale and user guide." Guide prepared by Gillian Potter, Zoe Morris and Prof Joanna Wardlaw*. Edinburgh: University of Edinburgh, 2015.
20. Duering M, Biessels GJ, Brodtmann A, et al. Neuroimaging standards for research into small vessel disease—advances since 2013. *Lancet Neurol* 2023; 22(7): 602–618.
21. Potter GM, Doubal FN, Jackson CA, et al. Enlarged perivascular spaces and cerebral small vessel disease. *Int J Stroke* 2015; 10(3): 376–381.
22. Cole JH, Poudel RPK, Tsagkrasoulis D, et al. Predicting brain age with deep learning from raw imaging data results in a reliable and heritable biomarker. *NeuroImage* 2017; 163: 115–124.
23. Karatzoglou A, Smola A, Hornik K, et al. Kernlab—An S4 package for kernel methods in R. *J Stat Softw* 2004; 11(9): 1–20.
24. Sati P, Oh J, Constable RT, et al. The central vein sign and its clinical evaluation for the diagnosis of multiple sclerosis: A consensus statement from the North American Imaging in Multiple Sclerosis Cooperative. *Nat Rev Neurol* 2016; 12(12): 714–722.
25. Absinta M, Sati P, Masuzzo F, et al. Association of chronic active multiple sclerosis lesions with disability in vivo. *JAMA Neurol* 2019; 76(12): 1474.
26. Geurts JJG, Roosendaal SD, Calabrese M, et al. Consensus recommendations for MS cortical lesion scoring using double inversion recovery MRI. *Neurology* 2011; 76(5): 418–424.
27. Maggi P, Bulcke CV, Pedrini E, et al. B cell depletion therapy does not resolve chronic active multiple sclerosis lesions. *eBioMedicine* 2023; 94: 104701.
28. Schilling S, Tzourio C, Dufouil C, et al. Plasma lipids and cerebral small vessel disease. *Neurology* 2014; 83(20): 1844–1852.
29. King KS, Peshock RM, Rossetti HC, et al. Effect of normal aging versus hypertension, abnormal body mass index, and diabetes mellitus on white matter hyperintensity volume. *Stroke* 2014; 45(1): 255–257.
30. Ekker MS, Boot EM, Singhal AB, et al. Epidemiology, aetiology, and management of ischaemic stroke in young adults. *Lancet Neurol* 2018; 17(9): 790–801.

31. Koo TK and Li MY. A guideline of selecting and reporting intraclass correlation coefficients for reliability research. *J Chiropr Med* 2016; 15(2): 155–163.
32. Bechmann I, Galea I and Perry VH. What is the blood–brain barrier (not)? *Trends Immunol* 2007; 28(1): 5–11.
33. Cumurciuc R, Guichard JP, Reizine D, et al. Dilation of Virchow-Robin spaces in CADASIL. *Eur J Neurol* 2006; 13(2): 187–190.
34. Kolbe SC, Garcia LM, Yu N, et al. Lesion volume in relapsing multiple sclerosis is associated with perivascular space enlargement at the level of the basal ganglia. *AJNR Am J Neuroradiol* 2022; 43(2): 238–244.
35. Wang Z, Chen Q, Chen J, et al. Risk factors of cerebral small vessel disease: A systematic review and meta-analysis. *Medicine (Baltimore)* 2021; 100(51): e28229.
36. Kappus N, Weinstock-Guttman B, Hagemeier J, et al. Cardiovascular risk factors are associated with increased lesion burden and brain atrophy in multiple sclerosis. *J Neurol Neurosurg Psychiatry* 2016; 87(2):181–187.
37. Geraldes R, Esiri MM, DeLuca GC, et al. Age-related small vessel disease: A potential contributor to neurodegeneration in multiple sclerosis. *Brain Pathol* 2017; 27(6): 707–722.
38. Pantoni L. Cerebral small vessel disease: From pathogenesis and clinical characteristics to therapeutic challenges. *Lancet Neurol* 2010; 9(7): 689–701.
39. Caunca MR, De Leon-Benedetti A, Latour L, et al. Neuroimaging of cerebral small vessel disease and age-related cognitive changes. *Front Aging Neurosci* 2019; 11: 145.
40. Filippi M, Preziosa P, Arnold DL, et al. Present and future of the diagnostic work-up of multiple sclerosis: The imaging perspective. *J Neurol* 2023; 270(3): 1286–1299.
41. Absinta M, Nair G, Monaco MCG, et al. The "central vein sign" in inflammatory demyelination: The role of fibrillar collagen type I. *Ann Neurol* 2019; 85(6): 934–942.
42. Sinnecker T, Clarke MA, Meier D, et al. Evaluation of the central vein sign as a diagnostic imaging biomarker in multiple sclerosis. *JAMA Neurol* 2019; 76(12): 1446.
43. Al-Louzi O, Letchuman V, Manukyan S, et al. Central vein sign profile of newly developing lesions in multiple sclerosis: A 3-year longitudinal study. *Neurol Neuroimmunol Neuroinflamm* 2022; 9(2): e1120.
44. Cavallari M, Egorova S, Healy BC, et al. Evaluating the association between enlarged perivascular spaces and disease worsening in multiple sclerosis. *J Neuroimaging* 2018; 28(3): 273–277.
45. Wardlaw JM, Smith EE, Biessels GJ, et al. Neuroimaging standards for research into small vessel disease and its contribution to ageing and neurodegeneration. *Lancet Neurol* 2013; 12(8): 822–838.
46. Geraldes R, Esiri MM, Perera R, et al. Vascular disease and multiple sclerosis: A post-mortem study exploring their relationships. *Brain* 2020; 143(10): 2998–3012.
47. Wiseman SJ, Bastin ME, Jardine CL, et al. Cerebral small vessel disease burden is increased in systemic lupus erythematosus. *Stroke* 2016; 47(11): 2722–2728.
48. Alghanimy A, Work LM and Holmes WM. The glymphatic system and multiple sclerosis: An evolving connection. *Mult Scler Relat Disord* 2024; 83: 105456.
49. Fitzgerald KC, Damian A, Conway D, et al. Vascular comorbidity is associated with lower brain volumes and lower neuroperformance in a large multiple sclerosis cohort. *Mult Scler* 2021; 27(12): 1914–1923.
50. Franke K and Gaser C. Ten years of BrainAGE as a neuroimaging biomarker of brain aging: What insights have we gained? *Front Neurol* 2019; 10: 789.
51. Cole JH, Raffel J, Friede T, et al. Longitudinal assessment of multiple sclerosis with the brain-age paradigm. *Ann Neurol* 2020; 88(1): 93–105.
52. Denissen S, Engemann DA, De Cock A, et al. Brain age as a surrogate marker for cognitive performance in multiple sclerosis. *Eur J Neurol* 2022; 29(10): 3039–3049.
53. Brier MR, Li Z, Ly M, et al. "Brain age" predicts disability accumulation in multiple sclerosis. *Ann Clin Transl Neurol* 2023; 10(6): 990–1001.
54. Groeschel S, Chong WK, Surtees R, et al. Virchow-Robin spaces on magnetic resonance images: Normative data, their dilatation, and a review of the literature. *Neuroradiology* 2006; 48(10): 745–754.
55. Okar SV, Hu F, Shinohara RT, et al. The etiology and evolution of magnetic resonance imaging-visible perivascular spaces: Systematic review and meta-analysis. *Front Neurosci* 2023; 17: 1038011.
56. Schwartz DL, Boespflug EL, Lahna DL, et al. Autoidentification of perivascular spaces in white matter using clinical field strength T1 and FLAIR MR imaging. *NeuroImage* 2019; 202: 116126.
57. Dubost F, Yilmaz P, Adams H, et al. Enlarged perivascular spaces in brain MRI: Automated quantification in four regions. *NeuroImage* 2019; 185: 534–544.